Article

Kinetics of Transient End-to-End Contact of Single-Stranded DNAs

Kiyohiko Kawai, Hiroko Yoshida, Akira Sugimoto, Mamoru Fujitsuka, and Tetsuro Majima

J. Am. Chem. Soc., **2005**, 127 (38), 13232-13237• DOI: 10.1021/ja0524999 • Publication Date (Web): 02 September 2005

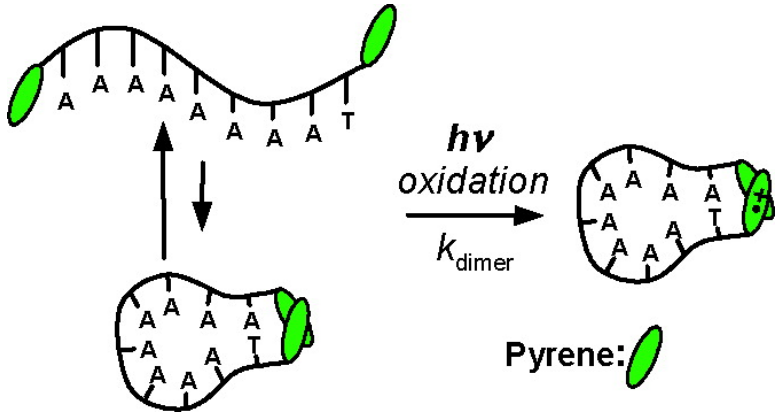

J|A|C|S
ARTICLES
Published on Web 09/02/2005

Kinetics of Transient End-to-End Contact of Single-Stranded DNAs

Kiyohiko Kawai,* Hiroko Yoshida, Akira Sugimoto, Mamoru Fujitsuka, and Tetsuro Majima*

Contribution from The Institute of Scientific and Industrial Research (SANKEN), Osaka University, Mihogaoka 8-1, Ibaraki, Osaka 567-0047, Japan

Received April 18, 2005; E-mail: kiyohiko@sanken.oskak-u.ac.jp; majima@sanken.osaka-u.ac.jp

Abstract: The formation of the pyrene (Py) dimer radical cation ($Py_2^{\bullet+}$) was used to measure the kinetics of the intrastrand end-to-end contact rates of single-stranded DNAs (ssDNAs) in the 10 nanoseconds to the tens of microseconds time range. ssDNAs labeled with Py at both ends with the lengths of 3, 6, and 9 mer were synthesized, and the two-photon ionization method was employed to generate a $Py^{\bullet+}$, which enables the measurements of the end-to-end contact rates from 10 ns. The formation rate of $Py_2^{\bullet+}$ depended on the length and the sequence of the ssDNAs, and about 1 order of magnitude faster rates were observed for the T-rich ssDNAs compared to those for the corresponding length of A-rich ssDNAs, showing that ssDNA made from adenines is much more rigid than that composed of thymidines. As for the T-rich ssDNAs, the formation of $Py_2^{\bullet+}$ attributed to the misfolded structures was also observed, which is consistent with the configurational diffusion model suggested by Ansari and co-workers.

Introduction

DNA is a dynamic structure in which several transient conformations appear depending on the time scale. Especially, the dynamics of single-stranded DNAs (ssDNAs) has attracted wide attention since the hairpin formation of single-stranded nucleic acids play an important role in many biological functions such as gene expression,[1,2] DNA recombination,[3] and DNA transcription.[4,5] Although the thermodynamic stability of hairpin loops[6,7] and the kinetics of the hairpin formation[7−11] have been intensively studied, the kinetics of the hairpin formation is still not fully understood.

Libchaber et al. described the dynamics of hairpin formation by a two-state model involving a fully folded hairpin and a random coiled state.[9,10] However, several experiments revealed a number of kinetic features that are not easily described by the simple two-state analysis. Ansari et al. explained the complex dynamics of hairpin formation by a configurational diffusion model which suggests the transient trapping in misfolded conformations early in the nucleation step.[7,8] It was suggested that the formation of the misfolded loops decreases the effective diffusion coefficient and slow hairpin formation. To examine this mechanism, Nau et al. measured the kinetics of the end-to-end collision rates in short ssDNAs. By using the oligonucleotide having a fluoroazophore (2,3-diazabicyclo-[2.2.2]-oct-2-ene: DBO) at one end and guanine at the other end, the end-to-end collision rates were measured through the fluorescence quenching of DBO by guanine.[11] The end-to-end collision rate of the short ssDNAs corresponding to the hairpin loop part was determined to be 1 order of magnitude faster ($\sim 10^6$ s^{-1}: measured for DBO-TTTT-G) than the kinetics of the hairpin formation ($\sim 10^5$ s^{-1}: measured by T-jump experiment for GGATAA-TTTT-TTATCC[8]). This indicates that the effective intrachain diffusion is significantly slowed during the hairpin formation, which is consistent with the configurational diffusion model, in which misfolded loops are presumed to slow the hairpin formation.

To further investigate the kinetics of the hairpin formation in more detail, measuring the rates of the end-to-end contact for ssDNAs longer than five bases, which are capable of forming a hairpin structure with a loop size of three or larger, was required. Although DBO show an extremely long fluorescence lifetime (420 ns) that is useful for the measurements of the dynamics of the biopolymers in the time range up to submicroseconds,[11−16] it is still not long enough for the

(1) McCaffrey, A. P.; Meuse, L.; Pham, T.-T. T.; Conklin, D. S.; Hannon, G. J.; Kay, M. A. *Nature* **2002**, *418*, 38.
(2) Zazopoulos, E.; Lalli, E.; Stocco, D. M.; Sassone-Corsi, P. *Nature* **1997**, *390*, 311.
(3) Roth, D. B.; Nakajima, P. B.; Menetski, J. P.; Bosma, M. J.; Gellert, M. *Cell* **1992**, *69*, 41.
(4) Soldatenkov, V. A.; Chasovskikh, S.; Potaman, V. N.; Trofimova, I.; Smulson, M. E.; Dritschilo, A. *J. Biol. Chem.* **2002**, *277*, 665.
(5) Catasti, P.; Chen, X.; Moyzis, R. K.; Bradbury, E. M.; Gupta, G. *J. Mol. Biol.* **1996**, *264*, 534.
(6) SantaLucia, J., Jr.; Hicks, D. *Annu. Rev. Biophys. Biomol. Struct.* **2004**, *33*, 415.
(7) Shen, Y.; Kuznetsov, S. V.; Ansari, A. *J. Phys. Chem. B* **2001**, *105*, 12202.
(8) Ansari, A.; Kuznetsov, S. V.; Shen, Y. *Proc. Natl. Acad. Sci. U.S.A.* **2001**, *98*, 7771.
(9) Goddard, N. L.; Bonnet, G.; Krichevsky, O.; Libchaber, A. *Phys. Rev. Lett.* **2000**, *85*, 2400.
(10) Bonnet, G.; Krichevsky, O.; Libchaber, A. *Proc. Natl. Acad. Sci. U.S.A.* **1998**, *95*, 8602.
(11) Wang, X.; Nau, W. M. *J. Am. Chem. Soc.* **2004**, *126*, 808.
(12) Huang, F.; Hudgins, R. R.; Nau, W. M. *J. Am. Chem. Soc.* **2004**, *126*, 16665.
(13) Huang, F.; Nau, W. M. *Angew. Chem., Int. Ed.* **2003**, *42*, 2269.
(14) Marquez, C.; Pischel, U.; Nau, W. M. *Org. Lett.* **2003**, *5*, 3911.
(15) Hudgins, R. R.; Huang, F.; Gramlich, G.; Nau, W. M. *J. Am. Chem. Soc.* **2002**, *124*, 556.

10.1021/ja0524999 CCC: $30.25

measurement of the end-to-end contact of ssDNAs longer than five bases which can form a double stranded stem.

Recently, we reported the use of the pyrene (Py) dimer radical cation ($Py_2^{\bullet+}$), in which the close interaction between Py and its radical cation ($Py^{\bullet+}$) leads to the formation of $Py_2^{\bullet+}$.[17,18] Two Pys were introduced at the end or at the internal site of the duplex DNA, and then the formation rates of $Py_2^{\bullet+}$ upon the one-electron oxidation by the reaction with $SO_4^{\bullet-}$ during the pulse radiolysis were measured. The DNA dynamics, which allows the interaction between $Py^{\bullet+}$ and Py, were investigated from the formation rates of the intramolecular $Py_2^{\bullet+}$, which is stabilized by the charge resonance (CR) between the two aromatics.[19−21] In this method, the long lifetimes of $Py^{\bullet+}$ and $Py_2^{\bullet+}$ allow us to measure the DNA dynamics in the time range from 1 μs to 1 ms. In this report, to measure the end-to-end contact rates of the ssDNAs, ssDNAs possessing Py at both ends were synthesized. Since pulse radiolysis is not convenient for measuring the kinetics on a time scale shorter than 1 μs due to the time required for the collisional process between Py and the oxidant $SO_4^{\bullet-}$ for the generation of a $Py^{\bullet+}$, we employed the two-photon ionization method to generate a $Py^{\bullet+}$, which enables the measurements of the end-to-end contact rates from 10 ns. The formation of $Py_2^{\bullet+}$ in DNA was measured during the laser flash photolysis of the doubly Py-modified ssDNAs, and the formation rate of the intramolecular $Py_2^{\bullet+}$ was discussed on the basis of the DNA dynamics which allows the interaction between $Py^{\bullet+}$ and Py.

Experimental Section

DNA Synthesis. 3′-Phospate CPG (2-[2-(4,4′-dimethoxytrityoxy)-ethylsulfonyl]ethyl-2-succinoyl)-long chain alkylamino-CPG) and all the other reagents for DNA synthesis were purchased from Glen Research. Cyanoethyl phosphoramidite of 1-pyrene butanol for the 5′-Py modification was synthesized as previously reported.[17,22−25] Synthesis of 4-pyrenylbutyl phosphoramidite of thymine for 3′-Py modification is described below. DNA used in this study were synthesized with Expedite 8909 DNA synthesizer (Applied Biosystems). After the automated synthesis, the Py-modified DNA was detached and deprotected by treating with 28% NH_3aq for 24 h at room temperature. Crude DNA was purified by reverse phase HPLC and lyophilized. All the DNA studied here were characterized by MALDI-TOFF mass spectra, and their concentrations were calculated from the absorbance of Py-moiety, where the absorbance of Py-AAA and Py-TTT, of which concentrations can be determined from the complete enzymatic digestion, were used as a standard for 5′-Py and 3′-Py, respectively.

Synthesis of Py-phosphoramidite (2) for 3′-Py Modification. 4-(1-Pyrenylbutyl *N*,*N*-diisopropylphosphoramidochloridite (**1**) was synthesized according to the reported procedures.[26] To a solution of 5′-*O*-(4,4′-dimethoxytrityl)-2′-deoxythymidine (273 mg, 0.5 mmol) in anhydrous dichloromethane (8 mL) was added diisopropylamine (0.8 mL) followed by the dropwise addition of a solution of **1** (440 mg, 1.0 mmol) in dichloromethane (20 mL), and the mixture was stirred for 4 days at room temperature. The reaction was quenched with methanol (2 mL), and the reaction mixture was washed with 5% aqueous solution of sodium hydrogen carbonate. The organic layer was dried over anhydrous sodium sulfate and evaporated to dryness. The residue was subjected to flash chromatography (ethyl acetate/triethylamine = 99/1 (v/v) to yield **2** (300 mg, 61% yield). ^{1}H NMR (270 MHz) ($CDCl_3$) δ 1.11−1.15 (m, 12H, *i*-Pr CH_3), 1.38 (s, 3H, C5 CH_3), 1.57−2.02 (m, 4H, $-CH_2-CH_2-$), 2.16−2.34 (m, 1H, H2′), 2.38−2.59 (m, 1H, H2″), 3.24−3.65 (m, 8H, H5′, H5″, *i*-Pr CH, Py-CH_2, P−O−CH_2), 3.74 (s, 3H, OCH_3), 3.75 (s, 3H, OCH_3), 4.10−4.13 (m, 1H, H4′), 4.56−4.70 (m, 1H, H3′), 6.32−6.44 (m, 1H, H1′), 6.74−8.25 (m, 23H, DMTr, Py, H6). FAB MASS (positive ion): *m*/*z* 950.

Fluorescence Spectra. Fluorescence spectra of Py-modified DNA were measured in aqueous solution in the presence of 20 mM Na phosphate buffer (pH 7.0) at a strand concentration of 4 μM at 23 °C on a Hitachi 850 spectrofluorometer.

Laser Flash Photolysis. The experiments were carried out at 23 °C for ssDNA in sodium phosphate buffer (20 mM, pD 7.0) in D_2O. All samples were purged with N_2O (unless otherwise mentioned). The third-harmonic oscillation (355 nm, full width at half-maximum of 4 ns, 20 mJ per pulse) from a Q-switched Nd:YAG laser (Surelight, Continuum, Santa Clara, CA) was used to excite Py. A xenon flash lamp (XBO-450, Osram, Berlin) was focused into the sample solution as the probe light for the transient absorption measurement. Time profiles of the transient absorption in the UV−visible region were measured with a monochromator (G250, Nikon) equipped with a photomultiplier (R928, Hamamatsu Photonics, Hamamatsu City, Japan) and digital oscilloscope (TDS-580D, Tektronix). Similarly, transient absorption in the NIR region were measured with a monochromator (SG-100, Koken) equipped with a fast InGaAs PIN photodiode equipped with an amplifier (Thorlabs, PDA255) and digital oscilloscope. All the transient absorption measurements were performed with single-shot irradiation (one pulse for one sample).

Fluorescence Lifetime Measurements. Time-resolved fluorescence spectra were measured by the single-photon counting method using a streakscope (Hamamatsu Photonics, C4334-01) equipped with a polychromator (Acton Research, SpectraPro150). Ultrashort laser pulse was generated with a Ti:sapphire laser (Spectra-physics, Tsunami 3941-M1BB, fwhm 100 fs) pumped with a diode-pumped solid-state laser (Spectra-Physics, Millennia VIIIs). For excitation of the sample, the output of the Ti:sapphire laser was converted to third harmonic generation (300 nm) with a harmonic generator (Spectra-Physics, GWU-23FL). The emission was monitored with a streak camera at wavelength 375−425 nm for the monomer emission, and at wavelength 450−565 nm for the excimer emission.

Results and Discussion

Synthesis of Doubly Py-Modified ssDNA. To attach Py at the 3′-end of ssDNA, Py-phosphoramidite derivative (**2**) was synthesized (Scheme 1). By using **2** and the 3′-phospate CPG as a solid support, Py was attached at the 3′-end of ssDNA. Modification of Py at the 5′-end was performed according to the reported procedures.[17,22−25] Although an alkaline labile phosphotriester was formed at the 3′-end during the synthesis, standard detach and deprotection procedures afford the final product without noticeable degradation due to the fast hydrolysis of the 3′-phosphate CPG moiety to give phosphodiester linkage.

Oxidation of Py by Two-Photon Ionization. To obtain the end-to-end contact rates faster than 1 μs, the two-photon ionization method was used instead of pulse radiolysis for the generation of $Py^{\bullet+}$. First, the two-photon ionization was tested

(16) Nau, W. M.; Wang, X. *ChemPhysChem* **2002**, *3*, 393.
(17) Kawai, K.; Miyamoto, K.; Tojo, S.; Majima, T. *J. Am. Chem. Soc.* **2003**, *125*, 912.
(18) Kawai, K.; Yoshida, H.; Takada, T.; Tojo, S.; Majima, T. *J. Phys. Chem. B* **2004**, *108*, 13547.
(19) Tsuchida, A.; Ikawa, T.; Yamamoto, M.; Ishida, A.; Takamuku, S. *J. Phys. Chem.* **1995**, *99*, 14793.
(20) Tsuchida, A.; Tsujii, Y.; Ohoka, M.; Yamamoto, M. *J. Phys. Chem.* **1991**, *95*, 5797.
(21) Kira, A.; Arai, S.; Imamura, M. *J. Chem. Phys.* **1971**, *54*, 4890.
(22) Mann, J. S.; Shibata, Y.; Meehan, T. *Bioconjugate Chem.* **1992**, *3*, 554.
(23) Takada, T.; Kawai, K.; Tojo, S.; Majima, T. *J. Phys. Chem. B* **2003**, *107*, 14052.
(24) Kawai, K.; Takada, T.; Tojo, S.; Majima, T. *Tetrahedron Lett.* **2002**, *43*, 8083.
(25) Kawai, K.; Takada, T.; Tojo, S.; Ichinose, N.; Majima, T. *J. Am. Chem. Soc.* **2001**, *123*, 12688.
(26) Lee, S.; Winnik, M. A.; Whittal, R. M.; Li, L. *Macromolecules* **1996**, *29*, 3060.

Scheme 1

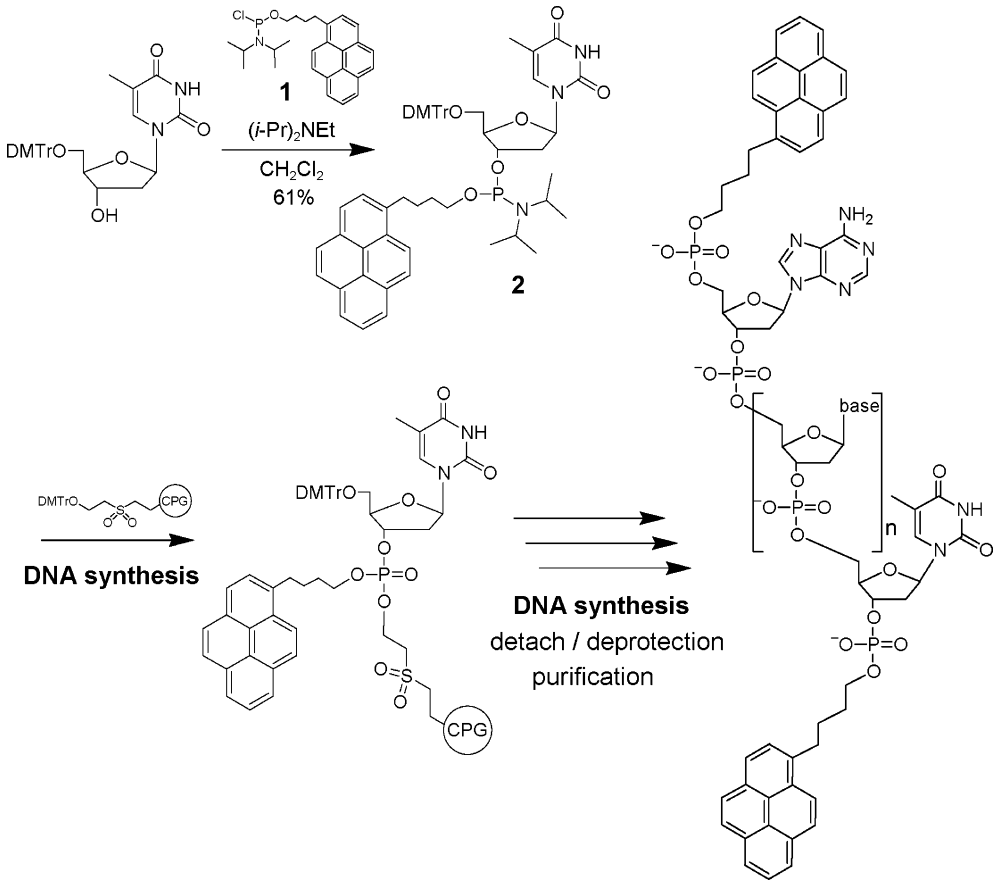

for the singly Py-modified 5′-Py-A. The photoirradiation of 5′-Py-A with a 355-nm laser pulse (fwhm = 4 ns, 20 mJ/pulse) under Ar-purged conditions lead to the formation of absorption bands at 470 and 630 nm immediately after the flash. These two absorption bands were assigned to $Py^{\bullet+}$ and a solvated electron (e_{aq}^-), respectively, demonstrating the successful electron ejection from Py to the solvent water during the excitation.[27] The transient absorption of e_{aq}^- decayed in about 1 μs under Ar, and it decayed within a laser pulse duration under N_2O-saturated condition (Figure 1). Thus, for the simplification of the kinetics, all the following transient absorption measurements were performed under N_2O-purged conditions. Under these conditions, the decay rate of $Py^{\bullet+}$ well correlated with the intermolecular formation rate of $Py_2^{\bullet+}$ with an absorption peak at 1550 nm (charge resonance band) which occurred in the time period of ~100 μs as shown in Figure 1.

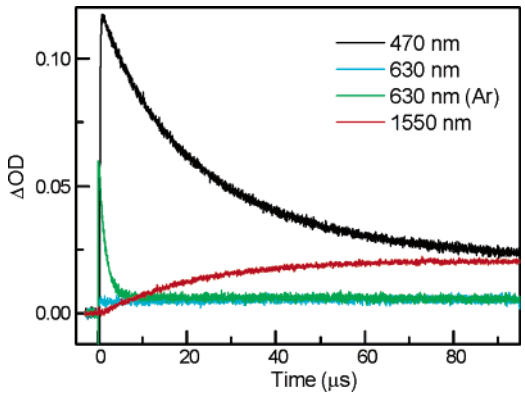

Figure 1. Time profiles of the transient absorptions assigned to $Py^{\bullet+}$ (470 nm, black), $Py_2^{\bullet+}$ (1550 nm, red), and e_{aq}^- (630 nm, cyan (green: under Ar)) during the two-photon ionization of N_2O-saturated D_2O solution of 5′-Py-A during the 355-nm laser flash photolysis. Sample solution contained 100 μM 5′-Py-A and 100 mM *t*-BuOH in 20 mM Na phosphate buffer (pD 7.0).

Sequence Design of Doubly Py-Modified ssDNA. The two-photon ionization of Py was examined for several singly Py-modified ssDNA hexamers. Since the two-photon ionization efficiency of Py strongly depends on the lifetime of Py in the singlet excited sate (^{1}Py*), the fluorescence spectra were measured. Py-AAAAAA showed a strong fluorescence emission around 370−460 nm, showing that ^{1}Py* has a long lifetime (Figure 2a). On the other hand, the fluorescence intensity of Py-TTTTTT was quite low due to the fast electron transfer and recombination reactions between T.[28−36] It has been well investigated that, in contrast to T, A does not act as a quencher of the fluorescence of alkylated pyrene derivatives.[28−36] Interest-

(27) Shafirovich, V. Y.; Dourandin, A.; Luneva, N. P.; Geacintov, N. E. *J. Phys. Chem. B* **1997**, *101*, 5863.
(28) Geacintov, N. E.; Zhao, R.; Kuzmin, V. A.; Kim, S. K.; Pecora, L. J. *Photochem. Photobiol.* **1993**, *58*, 185.
(29) Shafirovich, V. Y.; Courtney, S. H.; Ya, N.; Geacintov, N. E. *J. Am. Chem. Soc.* **1995**, *117*, 4920.
(30) O'Connor, D.; Shafirovich, V. Y.; Geacintov, N. E. *J. Phys. Chem.* **1994**, *98*, 9831.
(31) Shafirovich, V. Y.; Levin, P. P.; Kuzmin, V. A.; Thorgeirsson, T. E.; Kliger, D. S.; Geacintov, N. E. *J. Am. Chem. Soc.* **1994**, *116*, 63.
(32) Huber, R.; Fiebig, T.; Wagenknecht, H.-A. *Chem. Commun.* **2003**, 1878.
(33) Netzel, T. L.; Zhao, M.; Nafisi, K.; Headrick, J.; Sigman, M. S.; Eaton, B. E. *J. Am. Chem. Soc.* **1995**, *117*, 9119.
(34) Manoharan, M.; Tivel, K. L.; Zhao, M.; Nafisi, K.; Netzel, T. L. *J. Phys. Chem.* **1995**, *99*, 17461.
(35) Amann, N.; Pandurski, E.; Fiebig, T.; Wagenknecht, H.-A. *Angew. Chem., Int. Ed.* **2002**, *41*, 2978.
(36) Kawai, K.; Yokoohji, A.; Tojo, S.; Majima, T. *Chem. Commun.* **2003**, 2840.

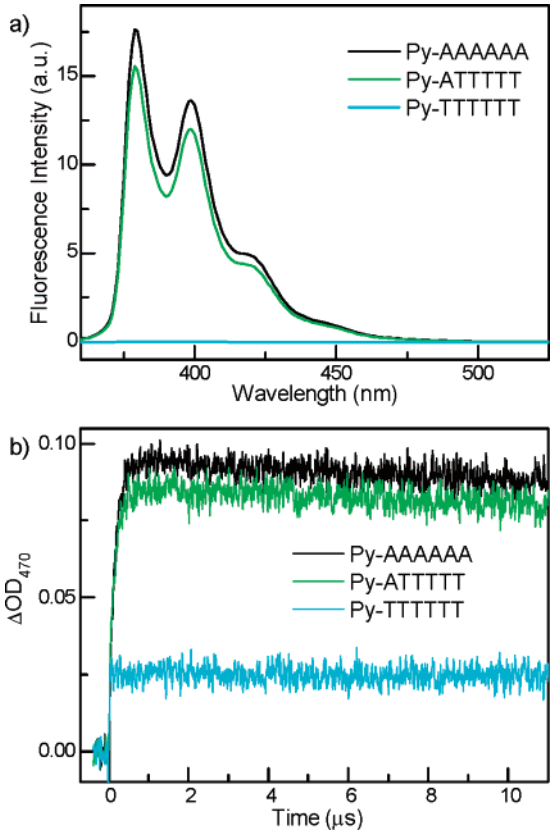

Figure 2. (a) Fluorescence spectra measured with excitation at 345 nm for singly Py-modified ssDNA hexamers. Sample solution contained 4 μM ssDNA in 20 mM Na phosphate buffer (pH 7.0). (b) Time profiles of the transient absorption of $Py^{\bullet+}$ monitored at 470 nm during the laser flash photolysis for N_2O-saturated D_2O solution of singly Py-modified ssDNA hexamers. Sample solution contained 25 μM ssDNA and 100 mM *t*-BuOH in 20 mM Na phosphate buffer (pD 7.0).

ingly, when T nearest to Py was replaced with A (Py-ATTTTT), the fluorescence intensity recovered to the level similar to that of Py-AAAAAA. The results for the laser flash photolysis of the ssDNA hexamers are shown in Figure 2b. Consistent with the fluorescence spectra, $Py^{\bullet+}$ was generated with a high yield for Py-AAAAAA, and that with a low yield for Py-TTTTTT. Here again, the yield of $Py^{\bullet+}$ recovered to the level similar to that of Py-AAAAAA by changing the T base adjacent to Py to A (Py-ATTTTT). Hence, to generate $Py^{\bullet+}$ in high yields, all the doubly Py-modified ssDNAs were designed so as to have T base at the 3′-end, and the A base at the 5′-end, in which photoirradiation mainly leads to the ionization of Py at the 5′-end.

End-to-End Contact Rates in A-Rich ssDNAs. The end-to-end contact rates in doubly Py-modified A-rich ssDNAs, Py-AA_nT-Py (n = 1, 4, 7), were examined. The photoirradiation of the doubly Py-modified ssDNA with a 355-nm laser lead to the formation of an absorption at 470 nm assigned to $Py^{\bullet+}$ within a laser pulse duration of 4 ns. Concomitant with the decay of $Py^{\bullet+}$, the formation of $Py_2^{\bullet+}$ with absorption peaks around 380 and 1500 nm was observed as shown in Figure 3a and 3b.[37] Since the intermolecular formation of $Py_2^{\bullet+}$ occurred on a much slower time scale for the singly Py-modified ssDNAs, and the intramolecular formation rates were independent of the concentration of DNA in the range of 12.5−50 μM for the doubly

(37) Apparent rise at 470 nm observed at early times was due to the imperfect subtraction of the Py fluorescence.

Scheme 2

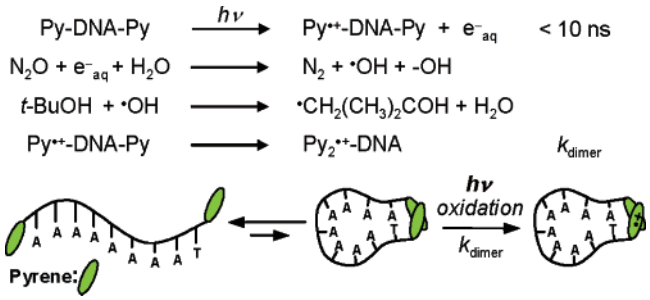

Py-modified ssDNA (see Supporting Information), the observed results are accounted for by intramolecular processes as shown in Scheme 2. The formation rate of $Py_2^{\bullet+}$ (k_{dimer}) was determined from the single-exponential fit of the time profiles in Figure 3c. The k_{dimer} depended on the length of the DNA and decreased by the factor of 4 and 2 as the length of the DNA increased from 3 to 6 and 9, respectively (Figure 3c and Table 1). As for the 3 and 6 mer ssDNAs, the length dependence of k_{dimer} was similar to the results of Nau et al. measured for DBO-AA-G ($5.4 \times 10^5\ s^{-1}$), and DBO-AAAA-G ($1.2 \times 10^5\ s^{-1}$),[11] except that a faster kinetics was observed here because of the flexible butyl linker used to attach Py. For the Py-AAT-Py, the fast formation of $Py_2^{\bullet+}$ within the laser duration was observed with a percentage of P_{static} (%) among the total $Py_2^{\bullet+}$ formed. This fast component was attributed to the population of the conformation in which two Pys locate close to each other at the nonoxidized state. The fluorescence spectra of Py-AA_nT-Py (n = 1, 4, 7) were shown in Figure 3d. A Py excimer emission was observed only for Py-AAT-Py. Since the formation of the Py excimer requires the close cofacial contact between the $^1Py^*$ and its neutral counterpart Py within the short lifetime of $^1Py^*$ in the context of ssDNA,[29−36] the Py excimer emission provides information about the population of the DNA conformation in which two Pys locate close to each other at the nonoxidized state. The fluorescence spectra were consistent with the formation of $Py_2^{\bullet+}$ within the laser duration observed for Py-AAT-Py.

End-to-End Contact Rates in T-Rich ssDNAs. Similarly, the end-to-end contact rates in the doubly Py-modified T-rich ssDNAs, Py-AT_nT-Py (n = 1, 4, 7), were investigated (Figure 4a). In all the sequences, the formation of $Py_2^{\bullet+}$ was observed to some extent immediately after the laser pulse due to the population of the conformation in which two Pys locate close to each other at the nonoxidized state, in line with the Py excimer emission observed for these ssDNAs as shown in Figure 4b. Time profiles of the formation of $Py_2^{\bullet+}$ for the T-rich ssDNAs were better fitted with a double exponential except for Py-ATT-Py. The rate of the fast component of k_{dimer} decreased with the increase in the length of DNA and was about 1 order of magnitude faster for the 6-mer ssDNA. This was explained by the stronger base-stacking interactions between the purines than those between the pyrimidines,[38,39] and was consistent with the results reported by Nau et al.[11] The end-to-end contact rates for the T-rich sequences were still much slower compared with those of the flexible polypeptides of similar length[40] due to the favorable π-stacking interactions between bases. The amplitude

(38) Ohmichi, T.; Nakano, S.-i.; Miyoshi, D.; Sugimoto, N. *J. Am. Chem. Soc.* **2002**, *124*, 10367.
(39) Guckian, K. M.; Schweitzer, B. A.; Ren, R. X. F.; Sheils, C. J.; Paris, P. L.; Tahmassebi, D. C.; Kool, E. T. *J. Am. Chem. Soc.* **1996**, *118*, 8182.

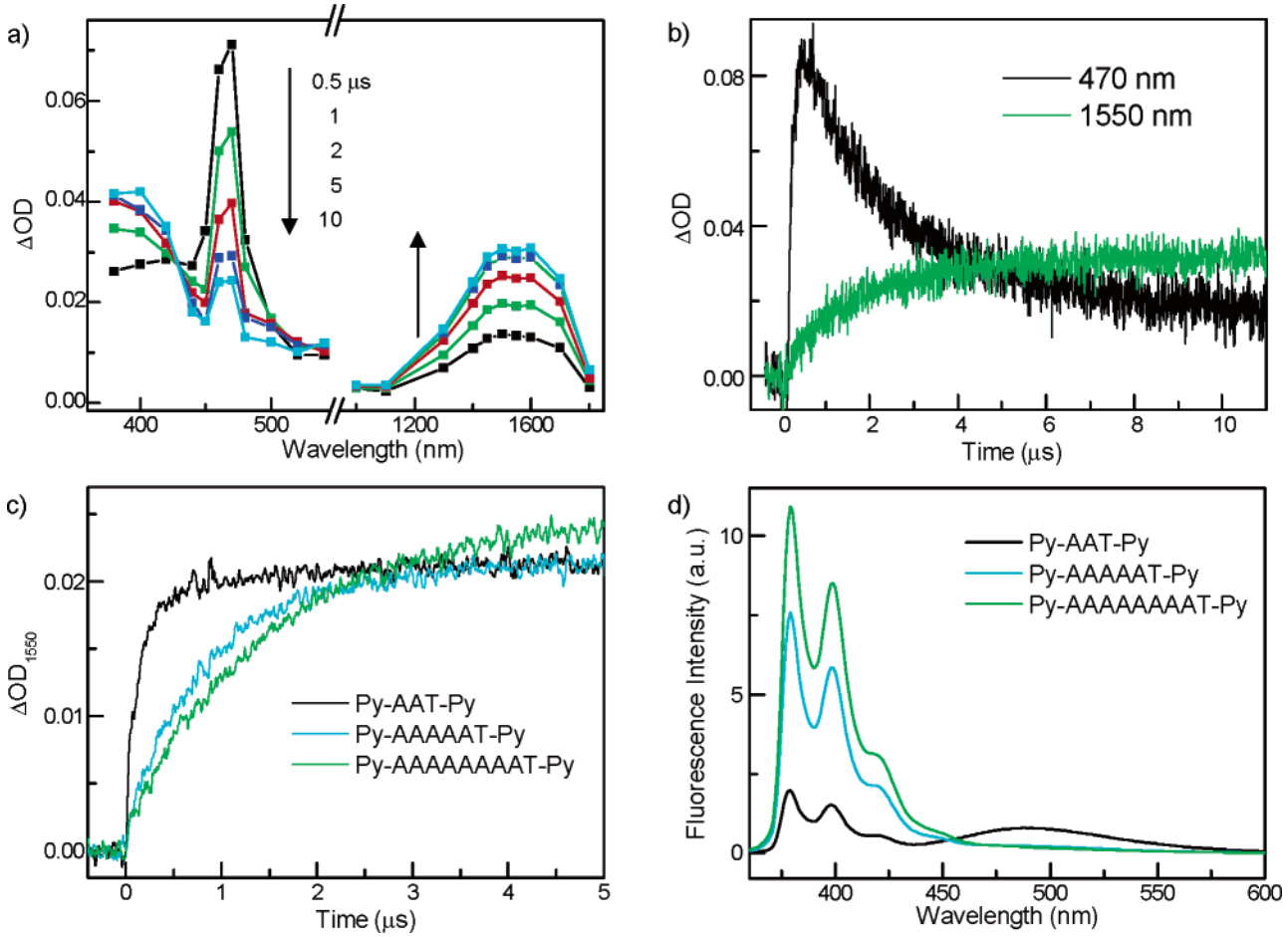

Figure 3. (a) The transient absorption spectra for Py-AAAAAT-Py observed at 0.5, 1, 2, 5, and 10 μs after the laser flash. (b) Time profiles of the transient absorption of $Py^{\bullet+}$ and $Py_2^{\bullet+}$ monitored at 470 and 1550 nm, respectively, during the laser flash photolysis of Py-AAAAAAAAT-Py. (c) Time profiles of the transient absorption of $Py_2^{\bullet+}$ monitored at 1550 nm during the laser flash photolysis for doubly Py-modified A-rich ssDNAs. Sample solution contained 25 μM ssDNA (12.5 μM in the case of (a)) and 100 mM *t*-BuOH in 20 mM Na phosphate buffer (pD 7.0). All samples were purged with N_2O. (d) Fluorescence spectra measured with excitation at 345 nm for doubly Py-modified A-rich ssDNAs. Sample solution contained 4 μM ssDNA in 20 mM Na phosphate buffer (pH 7.0).

Table 1. Formation Rate Constants (k_{dimer}) and Population of Each Component of Pyrene Dimer Radical Cation in Doubly Py-Modified ssDNAs

		k_{dimer} (10^6 s^{-1})[b]	
ssDNA	P_{static} (%)[a]	end-to-end contact	end-to-end contact via misfolded structure
Py-AAT-Py	32	5.1	–
Py-AAAAAT-Py	–	1.2	–
Py-AAAAAAAAT-Py	–	0.66	–
Py-ATT-Py	64	21 (36)	–
Py-ATTTTT-Py	42	16 (31)	1.2 (27)
Py-ATTTTTTTT-Py	27	3.3 (30)	0.20 (43)
Py-AATTTTTTT-Py	13	1.6 (19)	0.12 (68)
Py-AAATTTTTT-Py	15	0.74 (28)	0.10 (57)

[a] $P_{static} = \Delta OD_{t=10ns}/\Delta OD_{max}$. [b] Determined from the time profiles of transient absorption in Figures 3c and 4a. Numbers in parentheses are relative amplitudes of preexponential factors in exponential functions where the end-to-end contact rate constants and the P_{static} were normalized to sum up to 100%.

of the slower component of k_{dimer} increased with the increased length of ssDNA.

To gain some insight into the origin of the slower component of the k_{dimer}, ssDNAs Py-AATTTTTTT-Py and Py-AAATTTTTT-Py, which have a higher probability of forming intramolecular base-pairs, were additionally synthesized. Interestingly, the slower component of the k_{dimer} became significant for theses ssDNAs, and the rate of the fast component of k_{dimer} decreased and became close to that of Py-AAAAAAAAT-Py as the number of A bases increased. On the basis of these results, the slower component of the k_{dimer} was attributed to the misfolded structures in which base-pairs are incorrectly formed as suggested by Ansari and co-workers (Scheme 3).[8] The rate and the amplitude of the slower component of k_{dimer} were similar for Py-AATTTTTTT-Py and Py-AAATTTTTT-Py. Although the increase in the A bases increase the probability of base-pair formation, it increases the rigidity of the ssDNA that is not favorable for the misfolded structures at the same time. Since hairpin structures consisting of loops of thymidines are much more stable than those of adenines,[6,7] the slower component of k_{dimer} was only obvious for the T-rich ssDNAs.

Py Monomer and Excimer Fluorescence Lifetime Measurements. The kinetics of the collision between two Pys can also be examined by its excimer formation rates.[26,41−54] Since

(40) Krieger, F.; Fierz, B.; Bieri, O.; Drewello, M.; Kiefhaber, T. *J. Mol. Biol.* **2003**, *332*, 265.
(41) Siu, H.; Duhamel, J. *Macromolecules* **2004**, *37*, 9287.
(42) Okamoto, A.; Ichiba, T.; Saito, I. *J. Am. Chem. Soc.* **2004**, *126*, 8364.
(43) Kanagalingam, S.; Spartalis, J.; Cao, T.-M.; Duhamel, J. *Macromolecules* **2002**, *35*, 8571.
(44) Farinha, J. P. S.; Picarra, S.; Miesel, K.; Martinho, J. M. G. *J. Phys. Chem. B* **2001**, *105*, 10536.

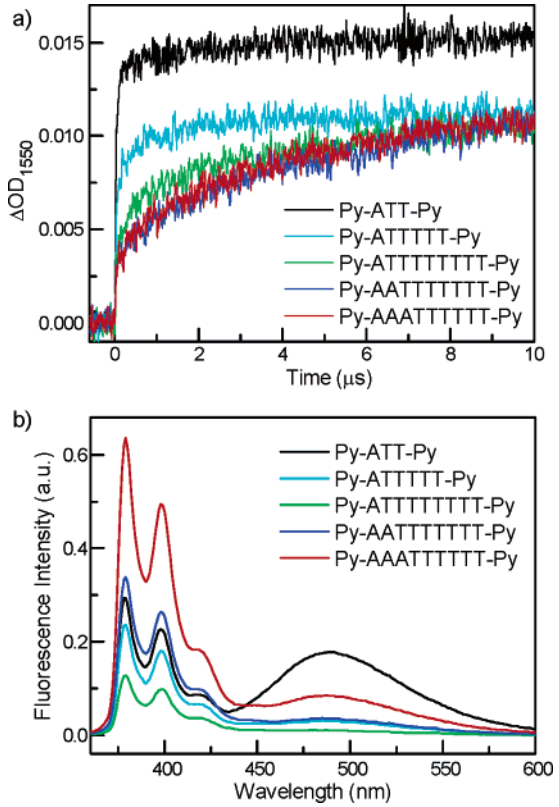

Figure 4. (a) Time profiles of the transient absorption of $Py_2^{\bullet+}$ monitored at 1550 nm during the laser flash photolysis for N_2O-saturated D_2O solution of doubly Py-modified T-rich ssDNAs. Sample solution contained 25 μM ssDNA and 100 mM *t*-BuOH in 20 mM Na phosphate buffer (pD 7.0). (b) Fluorescence spectra measured with excitation at 345 nm for doubly Py-modified T-rich ssDNAs. Sample solution contained 4 μM ssDNA in 20 mM Na phosphate buffer (pH 7.0).

Scheme 3

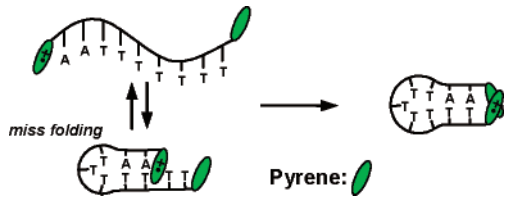

a strong excimer emission was observed for the short ssDNAs, Py-AAT-Py and Py-ATT-Py, their monomer and excimer fluorescence lifetimes were measured (see Table 2). In both cases, the monomer emission showed a double exponential decay. As for the excimer emission, a single-exponential decay lifetime which was different from that of the monomer emission was observed for Py-AAT-Py, showing that the excimer emission

Table 2. Monomer ($\tau_{monomer}$) and Excimer ($\tau_{excimer}$) Emission Lifetimes in Py-Modified ssDNA Trimers

ssDNA	$\tau_{monomer}$ (ns)[a]	$\tau_{excimer}$ (ns)[a]
Py-AAT-Py	0.37 (42), 12.3 (58)	19.8
Py-ATT-Py	0.74 (63), 7.62 (37)	1.53 (53), 7.62 (47)
Py-ATT	53.4	–

[a] Numbers in parentheses are relative amplitudes of preexponential factors in exponential functions.

originates from the ssDNA conformation in which two Pys associate close to each other at the ground state.[53] On the other hand, the decay was fitted with a double exponential for Py-ATT-Py, and the decay time of the slower component was identical to the decay of the slower component of the monomer emission. The fluorescence lifetime was also measured for the singly Py-modified Py-ATT, and the obtained monomer emission lifetime was much longer compared to that of Py-AAT-Py in which electron-transfer quenching by T is a bit weaker and no dynamic formation of the excimer was observed. These results indicate that Py at the 3′-end significantly contributes on the shortening of the monomer emission lifetime of Py at the 5′-end, probably through energy transfer from 5′-^{1}Py* to 3′-Py, followed by fast electron-transfer quenching of 3′-^{1}Py* by nearby T. Hence, it is a rather complicated subject to determine the association rates of Pys by means of the fluorescence lifetime measurements in this system, showing that the measurement of the formation rates of $Py_2^{\bullet+}$ may serve as an alternate method to measure the intramolecular contact of Pys in the context of DNA.

Conclusions

Two Pys were attached at both ends of ssDNA, and the formation of $Py_2^{\bullet+}$ was monitored by the CR band (1550 nm) during the laser flash photolysis. The long lifetimes of $Py^{\bullet+}$ and $Py_2^{\bullet+}$ offer the measurements of the processes in the time range up to milliseconds, enabling us to measure the end-to-end contact rates of ssDNAs longer than 5-bases that are normally not accessible to study by other methods. The formation rate of $Py_2^{\bullet+}$ depended on the length and the sequence of the ssDNAs, and was about 1 order of magnitude faster for the T-rich ssDNAs compared to the corresponding length of the A-rich ssDNAs. As for the T-rich ssDNAs, the slow formation of $Py_2^{\bullet+}$ attributed to the misfolded structures was also observed, supporting the configurational diffusion model suggested by Ansari and co-workers. So far, many doubly Py-modified molecules were synthesized and the dynamics of the corresponding parent molecules were measured through the formation rate of the Py excimer.[26,41−54] Our results clearly show that measurements of the formation rate of $Py_2^{\bullet+}$ will significantly expand the time scale of the available dynamics of such molecules over 1 ms which was inaccessible with the Py fluorescence lifetime measurement approaches.

Acknowledgment. This work has been partly supported by a Grant-in-Aid for Scientific Research on Priority Area (417), 21st Century COE Research and others from the Ministry of Education, Culture, Sports, Science, and Technology (MEXT) of the Japanese Government.

Supporting Information Available: Formation of $Py_2^{\bullet+}$ for the singly Py-modifed ssDNAs and its concentration dependency for the doubly Py-modified ssDNA. This material is available free of charge via the Internet at http://pubs.acs.org.

JA0524999

(45) Suzuki, Y.; Morozumi, T.; Nakamura, H.; Shimomura, M.; Hayashita, T.; Bartsh, R. A. *J. Phys. Chem. B* **1998**, *102*, 7910.
(46) Underhill, R. S.; Ding, J.; Birss, V. I.; Liu, G. *Macromolecules* **1997**, *30*, 8298.
(47) Eriksson, M.; Kim, S. K.; Sen, S.; Graslund, A.; Jernstrom, B.; Norden, B. *J. Am. Chem. Soc.* **1993**, *115*, 1639.
(48) Duhamel, J.; Yekta, A.; Hu, Y. Z.; Winnik, M. A. *Macromolecules* **1992**, *25*, 7024.
(49) Cheng, K. H.; Chen, S. Y.; Butko, P.; Van der Meer, B. W.; Somerharju, P. *Biophys. Chem.* **1991**, *39*, 137.
(50) Vauhkonen, M.; Sassaroli, M.; Somerharju, P.; Eisinger, J. *Biophys. J.* **1990**, *57*, 291.
(51) Eriksson, M.; Eriksson, S.; Norden, B.; Jernstroem, B.; Graeslund, A. *Biopolymers* **1990**, *29*, 1249.
(52) Sen, A. C.; Chakrabarti, B. *J. Biol. Chem.* **1990**, *265*, 14277.
(53) Winnik, F. M. *Chem. Rev.* **1993**, *93*, 587.
(54) Winnik, M. A. *Acc. Chem. Res.* **1985**, *18*, 73.